Electron excitations in the scattering of hydrogen and rare gas ions on Cu

O. Grizzi,[1] E. A. Sánchez,[1] S. Lacombe,[2] and V. A. Esaulov[2]

[1]*Centro Atómico Bariloche-CNEA, Instituto Balseiro-U.N.C., and CONICET, 8400 San Carlos de Bariloche, Río Negro, Argentina*
[2]*Laboratoire des Collisions Atomiques et Moléculaires (Unité Mixte de Recherche UMR 8625), bât 351, Université de Paris Sud, Orsay 91405, France*

We present results of an electron spectroscopy study of the electronic excitations produced in the scattering of 5–100 keV hydrogen and rare gas ions (He, Ne, and Ar) from single crystalline and polycrystalline Cu surfaces. For all the projectiles the electron spectra show structures in the region 13–50 eV, superimposed on a broad and intense background. Most of these structures are assigned to Cu excitations. We study the dependence of the position and intensity of the structures as a function of the energy and type of projectile, and of the incident and observation angles. We compare them with those observed in energy loss measurements induced by electrons. In the case of Ne scattering we observe additional peaks in the electron spectra around 20–35 eV which come from autoionization processes in Ne** scattered projectiles. In this case we also measured the production of Ne^+ and Ne^{++} versus projectile energy and discuss its relation with the Ne** autoionizing peaks.

I. INTRODUCTION

In this work we study the electron emission resulting from the interaction of rare gas ions (He^+, Ne^+, and Ar^+) and hydrogen with single and poly crystalline Cu surfaces in the 5 to 100 keV energy range. Two main processes are considered: projectile autoionization in the case of Ne scattering and surface electronic excitations for all the projectiles. The first process, i.e., production of excited states followed by autoionization,[1–11] has attracted considerable attention in relation to surface composition studies in low energy ion scattering LEIS and secondary ion mass spectroscopy (SIMS). An important factor affecting the accuracy of structure determination, especially when experiments with electrostatic analysis of particles are dealt with, is ion neutralization. Processes in which particles are reionized in violent collisions with surface atoms may significantly affect the fraction of backscattered ions. The understanding of both neutralization and ionization processes is thus of importance for the correct use of analytical techniques. For the systems studied here, the effect of autoionization is observed solely during Ne^+ scattering.

The understanding of surface electronic excitations under ion and electron bombardment and in particular of the excitation of surface and bulk plasmons has significantly progressed over the last years as a result of many experimental and theoretical works.[12–34] In general, surface plasmons have been studied using electron or photon excitation. Plasmon excitation also occur in the stopping of fast ions as a result of direct or indirect excitation and it has been recently shown that a plasmon assisted neutralization is an important process (see for example a recent survey by Baragiola *et al.*[27]). A good part of the work on plasmon excitation by ions has been performed on Al surfaces, which are characterized by an energy loss function with a simple behavior, i.e., dominated by a well-defined collective excitation. Studies of surface excitations by ions on other surfaces with more complex

electron structures (transition and noble metals for example) are scarce.

In the following we shall briefly summarize some results of earlier studies relevant to the work described here. The production of autoionizing states of Ne in collisions with Na, Mg, Al, and Si surfaces has been extensively studied in the past 20 years.[1–9] Most of these studies were performed in the low keV energy range. Strong differences with the gas-phase case,[35] concerning the type of excited states produced, have been observed. Amongst these is the existence of only two major lines attributed to the decay of Ne**$2p^4(^3P)3s^2$ and $2p^4(^1D)3s^2$, and the predominance of the triplet core state over the singlet core state.[1,3–9] The fact that the lowest $3s^2$ states and not other excited states are strongly populated has been explained in terms of the binding energies of the electrons in these states with respect to the work function of the metal. Some other autoionizing lines have also been observed[4,7] at low keV energies with a typical intensity of almost two orders of magnitude smaller than the main lines. Recently, we presented[9] a study of Ne autoionizing state production on a Al(111) surface in an extended energy range up to 50 keV and under grazing incidence. It was shown that the energy dependence of the production of the series of low intensity peaks is quite different from that of the two main peaks due to the $2p^43s^2$ autoionizing states. The secondary lines appear at higher energies and become very important at tens of keV. As discussed previously[7,9] from the three possible parent core configurations for the secondary lines the $2s^22p^4$ core had been ruled out because of their low binding energy. In high velocity collisions these may be populated more efficiently because of parallel velocity effects,[36] which would also result in a different energy dependence of their production. The other two possibilities, i.e., configurations with a $2s$ vacancy $2s2p^5nl$, $2s2p^6nl$ and configurations $2s^22p^3nln'l'$ could both, in principle, account for several of the secondary lines. Nevertheless, existing data[8] on photon

emission in this energy range, clearly shows that states with a $2s$ vacancy $2s2p^5(^1P, ^3P)nl$ and $2s2p^6nl$ are indeed excited at high energies. Concerning this last aspect, an interesting example is provided by the Ne-Cu interaction,[10] where the scattered Ne^+ fraction shows a steplike increase when the Ne incident energy exceeds a threshold at about 4 keV (Refs. 10, 11). This behavior was correlated with enhanced energy losses, the appearance of scattered Ne^{2+} particles and the detection of Ne Auger electrons. The ensemble of these phenomena was attributed[10] to innershell $2s$ vacancy creation in Ne during close collision with Cu, resulting in Ne excited states that reionize by Auger autoionization. It was suggested[10] that this process onsets at high energies since it requires sufficiently short internuclear distances for $2s$ excitation. In the present work we extend the investigation of Ne-Cu collisions to a wider energy range (up to 50 keV), and for smooth and rough surfaces (both single crystal and polycrystal Cu). Above 10 keV we observe production of other structures, which are assigned to $Ne^{**}2s2p^5nl$ and $2s2p^6nl$ states.

Collective electronic excitations of surfaces and in particular plasmon excitation in ion surface scattering has been the object of a large number of works.[13,14,17,19–21,23–34] Experimentally, ion induced plasmon excitation may be studied by observation of electrons or photons resulting from their decay. Radiative decay of surface plasmons can occur for some degree of surface roughness, which allows coupling of surface plasmon field to electromagnetic field of light. Radiative decay of surface plasmons during ion bombardment was reported in Ref. 37 and more recently for the Ag case.[33] Most recent experimental studies have focussed on the identification of structures observable in derivatives of secondary electron spectra resulting from ion (H, He, Ne, Ar) scattering on Al, ascribable to plasmon decay.[27] These structures have been attributed to surface and bulk plasmon excitation and most recently there appears to be indication of multipole plasmon excitation.[27] For the case of Al, both plasmon decay structures are clearly observed under electron irradiation, where a correlation between the energy loss peaks seen close to the elastic peak and the structures due to plasmon decay can be established.[27,34] For Cu surfaces, structures in the electron spectra in the region of 10–15 eV were observed by the Utrecht group and attributed to potential emission in the case of He projectiles,[38] plasmon decay for H^+ projectiles,[26] and to diffraction effects.[29,39] In the present work we observe for all the projectiles (H^+, He^+, Ne^+, Ar^+, and e^-) structures in the energy range from 13 to 50 eV, which appear for both single and polycrystalline Cu, and have little dependence on incident and observation angles. We discuss the origin of these structures based on energy loss experiments induced by electron bombardment and previous interpretations of the corresponding electron losses. In the following section we give a brief description of the experimental procedure and then present and discuss our experimental results.

II. EXPERIMENTAL DETAILS

The experiments were conducted in an UHV chamber working at 3×10^{-10} Torr (with the beam line on). The ions
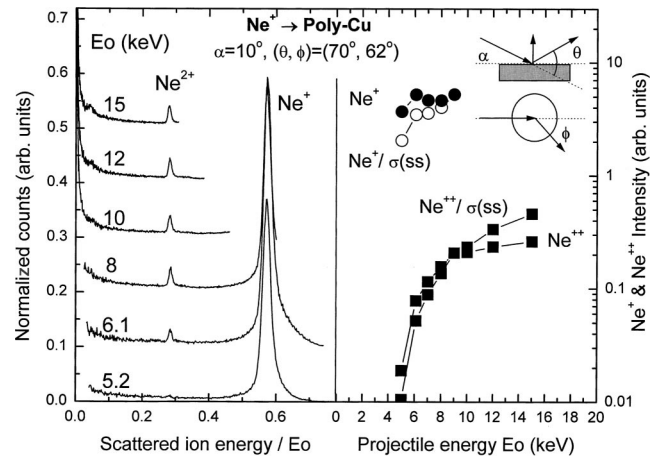
FIG. 1. (a) Ion energy spectra obtained for Ne^+ scattering off a polycrystalline Cu surface. The spectra are normalized and shifted vertically to ease the observation. Note the presence of Ne^{2+} above 5 keV. (b) Plots of the Ne^+ and Ne^{2+} intensities versus projectile energy, and of these values divided by the cross section for single scattering $\sigma(ss)$ at the measured angle. The inset shows the angle notation.

were generated in a radio frequency source, mass selected and collimated to better than 0.1°. The scattered ions and the emitted electrons were analyzed with a custom-made[40] cylindrical mirror analyzer working at 1% energy resolution and $\pm 1°$ angular resolution. Measurements of ions and electrons are carried-on separately, since they require different polarities in the analyzer voltages. The inner cylinder of the analyzer rotates around its main axis allowing measurements in a wide range of observation angles.[40] For the present measurements the incident angle (α) was varied from 1° to 10° with respect to the surface plane with the azimuthal orientation selected random. The observation angle was varied in a wide range; in each spectrum it is defined by the angles θ and ϕ, with θ the scattering angle, i.e., measured from the ion beam direction, and ϕ from the scattering plane (inset of Fig. 1). The spectra shown are not corrected for the transmission function of the analyzer, which is approximately proportional to the energy. In addition to the spectroscopic data, for the Ne-Cu case we acquired some time of flight spectra for neutrals plus ions and only neutrals scattered at 107°. The purpose of these measurements was to obtain the scattered Ne^+ ion fraction and the Ne^{**} autoionizing line intensity under the same experimental conditions (projectile incidence and surface roughness).

The preparation of the Cu (100) and Cu polycrystalline surfaces was performed by repeated cycles of 20 keV grazing Ar bombardment and annealing at 450 °C. The azimuthal orientation of the surface was continuously changed during the Ar bombardment. This method produces a surface topography that is strongly dependent on the incident angle of the Ar beam. At 0.5°–2° flat surfaces can be obtained while incident angles larger than 10° produces a rough surface. The cleaning of the surface was verified with Auger electron spectroscopy before and after performing the measurements.

III. RESULTS

A. Ionization and excited state production in Ne scattering

1. Ion scattering

To study the excitation and ionization processes for Ne^+ projectiles we performed ion scattering measurements, some ion fraction measurements and finally an electron spectroscopy study focused on the production of autoionizing states. Figure 1(a) shows ion scattering spectra plotted versus E/E_o (E: scattered ion energy, E_o: primary ion energy) for polycrystalline Cu. The spectra are normalized to the incident current and shifted vertically to facilitate the observation. Note that in this scale the spectra appear aligned but it results in a compression of the peaks. The high-energy peak corresponds to scattered Ne^+ while the peak that appears at $E/E_o = 0.285$ is due to Ne^{2+}. Figure 1(b) shows the intensity (area of the peaks) and also the intensity divided by the single scattering cross section corresponding to a scattering angle of 75° (the direction of observation). The dependence of the Ne^+ intensity with projectile energy is similar to that measured by Buck *et al.*,[10] i.e., it increases in the low energy region, from 5 to 6 keV in our case (we did not reach the sharp rise at 4 keV seen in their measurements) and then becomes less dependent on projectile energy. As may be seen, in agreement with the measurements of Ting Li and MacDonald,[11] the Ne^{2+} peak appears clearly in the ion spectra above 5 keV. The intensity of Ne^{2+} increases rapidly till about 8 keV and then keeps increasing more gradually (above 8 keV the height of the peaks becomes approximately constant but they become broader). This intensity divided by the cross section for single scattering, which should be approximately proportional to the scattered ion fractions, shows a stronger dependence on projectile energy and has a threshold of about 4.5 keV.

Figure 2 shows time of flight spectra measured for 10 keV Ne^+ scattering from poly-Cu. In this case, both neutral plus ions and only neutral are measured; the ion spectrum was obtained from their difference. The angle of incidence was set at 10° with respect to the surface plane and the observation at a scattering angle (θ) of 107°. If we integrate the full spectrum, corresponding to single and multiple collision sequences, the ion fraction is small, about 13%. On the other hand, the ion fraction for the single collision case is much higher. If we assume that the ion peak comes mainly from the first layer and integrate the neutrals above a smooth background we obtain an ion fraction value around 60% which is in good agreement with the value measured by Buck *et al.*[10] for first layer scattering.

2. Electron spectroscopy

Typical electron energy spectra due to Ne^+ incident on Cu are shown in Fig. 3 for 3.5, 10, and 20 keV incident ion energies. The spectra are composed of a broad background on which are superposed small structures whose intensity increases somewhat with increasing ion energy. In this figure a smooth background was also subtracted to obtain a better view of the structures, which are assigned to decay of autoionizing states of Ne**. Note that these appear shifted at
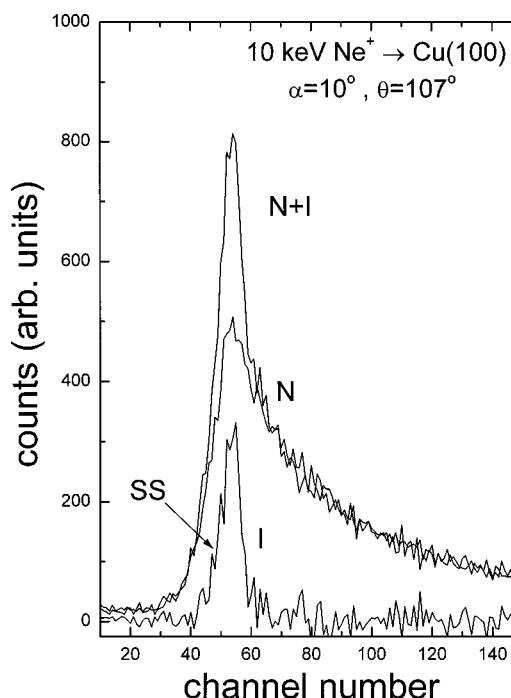
FIG. 2. Time of flight spectra for neutrals plus ions ($N+I$), only neutrals (N) and only ions (I) produced in 10 keV Ne^+ scattering off a clean Cu (100) surface at 107°. The neutral spectrum is broad and comes mainly from multiple scattering sequences, while the ion spectrum is much narrower with a larger contribution from single scattering (SS) collisions.

different ion energies. This shift is due to kinematic or Doppler effects[3–10] due to the emission from a moving ion. This effect also leads to some broadening of the spectral features in the laboratory frame of reference.

These structures are similar to what we observed in our earlier studies of Ne scattering on Al and other targets as mentioned above. The structures are better defined at grazing incidence and at the higher energies where we can clearly distinguish four peaks instead of the three structures observed previously.[10]

We also observed that the intensity of these structures and their width changes as a function of surface roughness, an effect we discussed in detail recently for the Al case.[9,41] An example is shown in Fig. 4 for 10 keV collisions, where we can see a broader structure than in Fig. 3, which was obtained after a short period ($\sim$30 min) of grazing sputtering with the Ne beam of a previously roughened surface with 20 keV Ar bombardment at normal incidence. A better flat surface (obtained by grazing sputtering for several hours and annealing) gives no structures at all, as it can be seen in the spectrum labeled "flat surface" (Fig. 4). In order to see reasonably well-defined Ne autoionizing structures we always had to roughen the surface by heavy Ar or Kr bombardment at large angles. This effect is related to the fact that for a flat surface the autoionizing atoms decay closer to the surface, at distances where the energy difference between the Ne** state level and the Ne^+ level is shifted with respect to the corresponding one at infinity due to image potential effects. For ion trajectories closer to the surface, the structures due to

Ne$^+ \rightarrow$ Cu(100)
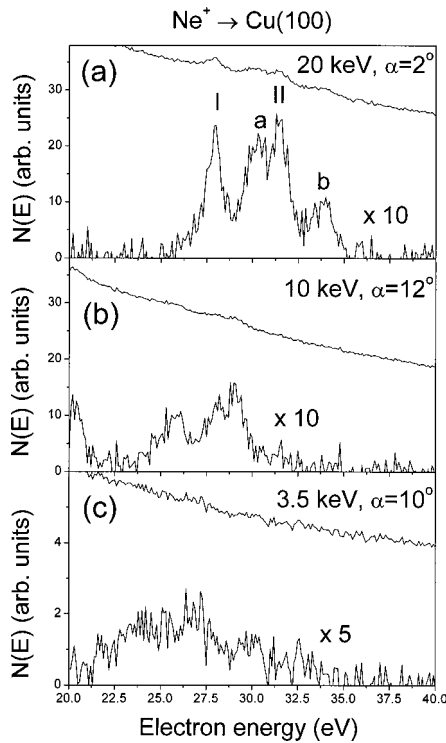
FIG. 3. Electron energy spectra produced in Ne$^+$ collisions with a rough Cu (100) surface. The observation angle was set at forward angles ($\theta = 35°$, $\phi = 10°$) to better define the Ne** autoionizing lines. Also shown in the figure is the spectrum after a smooth background subtraction. Note that at 3.5 keV the Ne** lines are barely observable.

Ne** autoionization become structured.[41,42] On a rougher surface decay occurs (on average) farther from the surface, the peaks become narrower and their position is closer to the one at infinite separation, i.e., the gas phase position. In case of Cu the flattening of the surface by the grazing ion beam was sufficient to broaden rapidly the Ne lines and make them disappear, an effect that is much more efficient than in Al, which could be related with a higher Cu sputtering yield.

By analogy to earlier work, the structures labeled I and II can be assigned to Ne** $2p^4$ (^3P) $3s^2$ and $2p^4$ (^1D) $3s^2$[1]
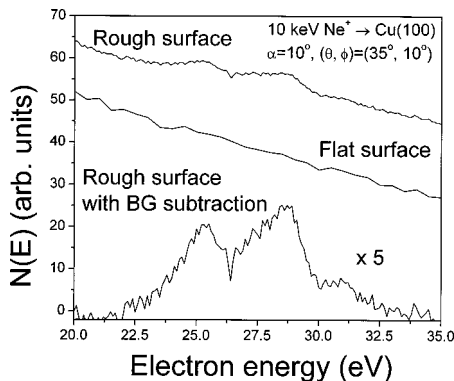
FIG. 4. Electron energy spectra produced in 10 keV Ne$^+$ collisions with a Cu (100) surface for two stages of surface roughness. Note that in the case of the flat surface the Ne lines are not observable.

deexcitation. Note that in the case of Cu, the singlet D appears to be more intense than the triplet P, which is not the case in Al, although it is closer to the behavior of Ne lines in gas phase collisions. This means that the core rearrangement process responsible of the dominance of the triplet P peak in Al is not so efficient in Cu. The features a and b are similar in intensity and position to the ones observed at these higher energy collisions in case of Ne scattering on Al.[9] As for Al we would assign these to the production of the Ne $2s$ vacancy states: $2s2p^5$ ($^1P, ^3P$) nl and $2s2p^6nl$. This assignment agrees with that proposed by Buck et al.[10] but does not imply that all excitations including the $2p^4$ core states must occur via the $2s$ vacancy production. The existence of Ne^{2+} (as evidenced in Fig. 1) and the fact that the autoionizing lines are so small, while the ion fractions (Fig. 2) are so large, suggest that autoionization is not the only channel responsible for the ion fractions, i.e., single and double ionization of Ne in the hard collision (after neutralization in the incoming part of the trajectory) may contribute to the scattered ion fraction.

It should be noted in this context that the Ne-Cu case tends to fit into a general trend. Indeed it is observed that Ne** $2p^4$ core states are most strongly excited in case of Ne scattering on Na. The intensity of production of these states at low energies then decreases as one goes from Na to Mg, Al, and finally Si. Excitation of $2p^4$ core Ne** states is most efficient at low energies for the quasisymmetric Ne-Na case as one would expect by analogy with gas phase collisions. The low intensity observed for the Cu case fits into this trend.

B. Cu surface excitations

Electron energy distributions produced during H$_2^+$, He$^+$, Ne$^+$, and Ar$^+$ scattering off Cu(100) and polycrystalline Cu surfaces were measured over a large energy range, from 5 to 50 keV, and for different incident and observation angles. Figure 5 shows some examples of these electron spectra, and the corresponding derivative spectra. In order to get a clean and smooth surface the Cu(100) sample was prepared by grazing ion bombardment and annealing. In this case, as described above, since the surface is sufficiently smooth, the Ne** autoionizing lines are absent. The polycrystalline Cu was cleaned by sputtering alone (without annealing).

Figures 5(a) and 5(b) show electron spectra produced by 50 keV H$_2^+$ and He$^+$ scattering off smooth Cu (100) and rough polycrystalline Cu, respectively. As we will see in following figures, measurements with H$^+$ show basically the same features than for H$_2$. For both projectiles we observe a large and asymmetric energy distribution of secondary electrons. Superimposed on the high-energy tail of these distributions there are several structures of lower intensity. There is a hump around 20 eV, which is clearly seen in the derivative spectrum (the energy positions indicated throughout the paper are those corresponding to the minimum in the derivative spectrum). For light projectiles we also observe the Cu Auger peak around 60 eV. In addition to these structures, some other structures in the range from 30 to 52 eV can also be observed. As opposed to the behavior of the peaks due to
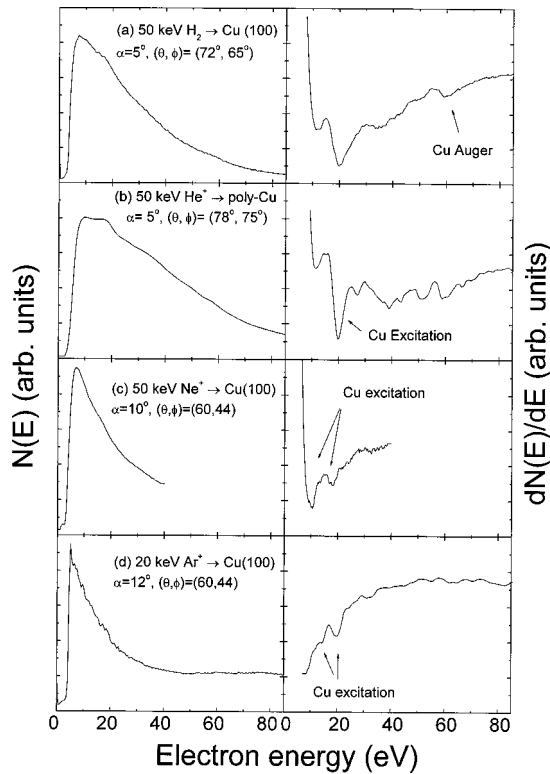
FIG. 5. Electron energy spectra and their first derivative produced in H_2^+, He^+, Ne^+, and Ar^+ collisions with single and polycrystalline Cu surfaces.

FIG. 6. First derivative of the electron energy spectra acquired with 20 keV H^+ scattering off the Cu(100) surface along different azimuthal orientations.

Ne** autoionizing states (seen only for rough surfaces Figs. 3 and 4) which show a considerable shift with projectile energy due to Doppler effect, these structures are approximately independent of projectile energy, and thus correspond to emission from the surface. For the heavier projectiles [Figs. 5(c) and 5(d)] the hump around 20 eV is observed with a weaker intensity. This is also the case for the Cu Auger line around 60 eV, which, as shown by Louchet *et al.*,[43] it is weakly excited for Ar projectiles.

Spierings[39] has also observed a similar hump in the electron spectra coming from crystalline Cu bombarded by H_2^+ and by He^+ at lower energies (below 5 keV). In their case the hump appears at a somewhat lower energy (around 15 eV). Another difference (in addition to the projectile energy range) is that their measurements were performed closer to the sample normal, while ours are far from the sample normal. The humps observed in the low energy region of the Cu electron spectra have received different interpretations, depending on the projectile type. For H_2 projectiles it was suggested that diffraction effects could account for the hump.[44] In the case of He^+ projectiles, a similar hump was attributed to potential electron emission,[38] while for protons it was attributed to plasmon decay.[26] More recently, shifts observed in the position of the hump and other considerations reinforced the diffraction model.[44,45] In order to identify the structures obtained in our experiments we performed measurements in a broad energy range, from 5 to 100 keV, in a broad range of observation angles, and for both crystalline [Cu(100)] and polycrystalline Cu surfaces. We also carried

out measurements under electron bombardment in order to correlate the energy loss structures around the elastic peak with the structures seen at low energies.

Figure 6 shows the derivative of electron spectra acquired with 20 keV protons hitting the Cu(100) surface at 5° incidence, and at different azimuths. The observation angle was fixed at $(\theta,\phi)=(60°,44°)$. The azimuth 0° is not correlated to a particular crystallographic axis, it corresponds to a random azimuth. We observe that within the experimental statistics the hump at ~20 eV has little or no dependence on the azimuthal direction of incidence. Other measurements at different azimuths, or with different projectiles showed the same behavior with azimuthal direction. From this measurement one can conclude that the hump seen in our measurements cannot come from a diffraction effect. However, this does not necessarily exclude the possibility of having diffraction effects for this source of electrons at other angles of observation, or on other Cu faces, as could be the case in the measurements near the surface normal by the Utrecht group.[38,39,44] Although the intensity of this hump decreases with decreasing projectile energy it could be followed down to our lower energies (5 keV). In the derivative mode, the electron spectra also show a smaller structure centered around 13 eV.

Figure 7 shows spectra measured with 100 keV protons along a fixed azimuth, at the same observation angle $(\theta,\phi)=(60°,44°)$, but for different polar incident angles. Here, the main feature is an enhancement of all the structures for 1° incidence. In particular, the 13 eV becomes readily visible. At this high energies Auger electrons from Cu are strongly excited (peak at ~60 eV).
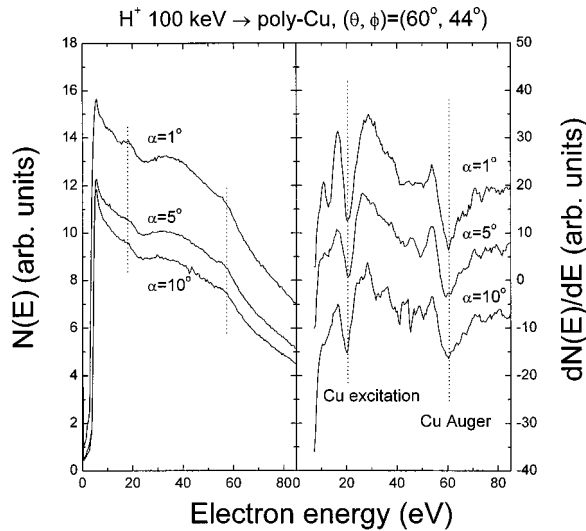
FIG. 7. Electron energy spectra and their first derivative produced in 100 keV H$^+$ collisions with the Cu polycrystalline surface acquired for different polar incident angles.

Figure 8 shows spectra in both the normal mode and in the derivative mode acquired also with 100 keV protons, but on polycrystalline Cu. In this case the incidence direction (polar and azimuthal) remains fixed and the observation angle is changed as is indicated in the figure. The hump at ~20 eV is also clearly seen at all the observation angles, with little dependence on angle. There are small variations in its shape and/or intensity, which might be due to statistics or to the strongly varying background. At more forward angles, i.e., closer to the ion specular direction (not shown), the structure at 20 eV is still present but it becomes more difficult to observe because of the rapid increase of the process of capture into continuum states of the projectile, which gives a very broad and intense structure, covering the range from 20 to 100 eV.[46,47]
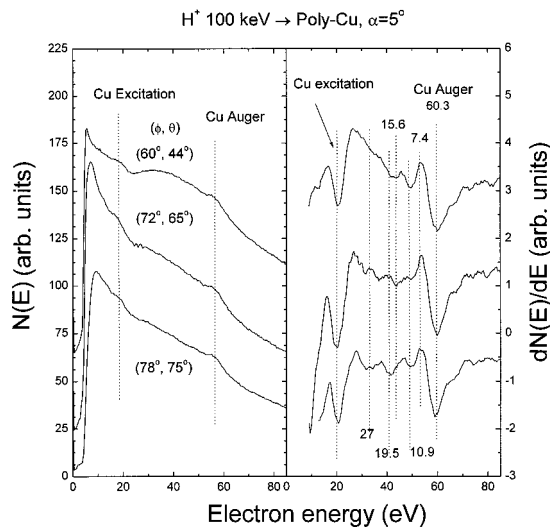
FIG. 8. Electron energy spectra and their first derivative produced in 100 keV H$^+$ collisions with the Cu polycrystalline surface acquired at different observation angles. The vertical lines in the derivative spectra indicate energy losses for 60 eV Auger electrons estimated from Fig. 9.
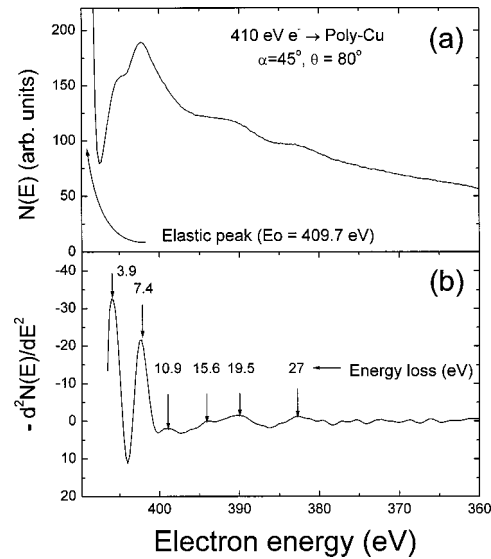
FIG. 9. Electron energy loss spectrum (a) and its second derivative produced by 409.7 eV electrons. The numbers in (b) indicate the observed energy losses $409.7 - E_m$, with E_m the position of the maximum in $-d^2N(E)/dE^2$.

From all the above results we can conclude that the observed structures are not a result of a particular diffraction effect. They cannot be attributed to Auger neutralization of a particular projectile since they are observed for different projectiles and essentially do not depend on observation angle, as should be the case for Auger neutralization in grazing scattering at intermediate energies.[48] The structures could then be attributed to excitations of the Cu surface, either to decay of a collective mode (plasmon) or to single (interband) electron excitations. In order to attempt an identification of the structures and to see which of them were present under electron bombardment we carried on a series of measurements with electrons hitting two different polycrystalline Cu surfaces, with energies in the range 200–2000 eV, and in two different experimental setups. One of these setups is the same as the one used for ions, the other is a commercial μ-metal chamber equipped with standard surface science techniques. In particular this chamber has a hemispherical analyzer used for AES, XPS, and EELS. In this case the observation is at 10° from the sample normal.

EELS data acquired with 409.7 eV incident electrons is shown in Fig. 9. Figure 9(b) shows the second derivative $[-d^2N(E)/dE^2]$ as is the practice in the presentation of EELS data. The $-d^2N(E)/dE^2$ spectrum shows a complex loss structure characterized by several maxima. The positions of these maxima are in good agreement with those measured previously (Table I). The assignment of these structures in the loss spectrum is not straightforward as is the case for Al, and has been the subject of many discussions concerning their collective or interband character, and the surface versus bulk relative contributions. Chiarello et al.[49] attributed the measured peaks in $-d^2N(E)/dE^2$ mainly to collective excitations. The loss feature at 19.5 eV was attributed to collective excitation of coupled s and d Cu electrons while the 27 eV feature was attributed to interband transitions.[50] The first

TABLE I. Position of the maxima in $-d^2N(E)/dE^2$ spectra of Fig. 9 corresponding to the energy losses suffered by 410 eV electrons incident on a polycrystalline Cu surface. Values from other works (Refs. 49, 51, 55) are also indicated.

	Energy position (eV)					
This work	4.0	7.4	10.9	15.6	19.5	27
Chiarello *et al.* (Ref. 49)	4.27	7.2	10.3	15.0	19.5	27.5
Ming-Cheng *et al.* (Ref. 55)	4.2	7.1			19.1	26.9
Papp (Ref. 51)	4.5	7.7	10.5		19.0	27.5

one showed a strong dependence on surface changes produced by adsorption[51] and it was therefore suggested that it contains a strong proportion of surface excitation.

Analysis of the real and imaginary parts of the dielectric function (ε) for Cu shows[52] that in contradistinction with the Al case, plasmons have unusual characteristics, in the sense that where the real part of ε is zero, the imaginary part of ε is large. The loss structures in the energy range from 10 to 50 eV, which are the ones of interest in our measurements because they can be related to the observed structures, come from relatively small variations in the real and imaginary (ε_1 and ε_2) parts of ε.[52,53] However, these small variations in ε_1 and ε_2 result in clear structures in the loss function Im $(-1/\varepsilon)$ around 20 and 27–30 eV.[53,54] Recent *ab initio* pseudopotential calculations[53] show that *s* electrons would generate a structure in the energy loss function around 12 eV. The inclusion of *d* electrons in the calculations results in a damping of the *s*-like collective oscillation and the appearance of a *d*-like double peak structure near 20 and 28 eV. Since these peaks occur at energies where ε_1 is close to zero, they are in the nature of collective excitations.[53] Transitions from *d* bands at about 2 eV below the Fermi energy to unoccupied states at ~23 eV above the Fermi energy also contribute and generate a peak in ε_2. According to the authors,[53] this combination of *d*-like collective excitations and interband electron-hole transitions results in a prominent double peak in the loss function.

Figure 10 shows electron spectra and their first derivatives induced by bombardment with 410 and 2300 eV electrons. The spectrum for 410 eV was acquired under the same experimental conditions than the spectrum of Fig. 9, that is, close to the sample normal. The other spectrum was acquired in the same chamber as the ion-induced spectra. The different relative intensity between the Cu Auger peak and the hump at 20 eV is partly due to the fact that the 410 eV spectrum was acquired with a constant pass energy (transmission of the analyzer approximately constant) while in the other case the transmission of the analyzer is approximately proportional to the energy. In both cases the hump appears at about the same energy than in the ion induced spectra shown in previous figures, showing that this feature is indeed a surface excitation and is not correlated to the type of projectile. In the case of the spectrum acquired with 2300 eV electrons, a smaller structure at about 13 eV can be observed. This structure at 13 eV was also observed in ion induced spectra (Figs. 5–8). Comparing the energy loss spectra (Fig. 9) and those of low energy electrons induced by electron bombard-
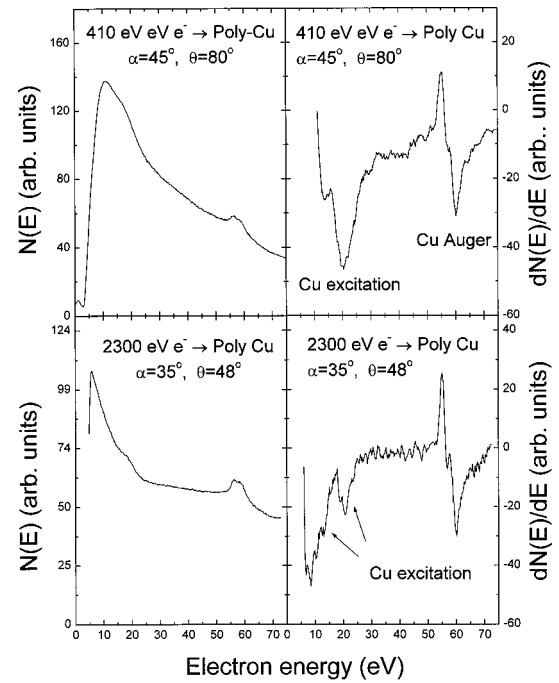
FIG. 10. Electron energy spectra and their first derivative produced in 409.7 and 2300 eV electrons colliding with two different Cu polycrystalline surfaces. The 2300 eV spectrum was acquired with the instrument used for the ion induced spectra shown in Figs. 3–8. The 409.7 eV spectrum corresponds to the low energy region of the spectrum of Fig. 9.

ment (Fig. 10) we can assign the 13 and 20 eV structures to the losses seen at 19.5 and 27 eV, respectively. If a 27 eV plasmon decays by transferring the energy to *d* electrons, the peak should have a maximum energy (corresponding to ejection of electrons lying at 2 eV below the Fermi energy) around $27 - W_{Cu} - 2 = 20.4$ eV, where $W_{Cu} = 4.6$ eV is the Cu work function. A minimum in the first derivative of the electron spectrum should appear close to this energy. Similarly, a plasmon of 19.5 eV should generate electrons of ~12.9 eV. These values are very close to the observed ones in the electron-induced spectra (Fig. 10). The structures seen in the ion spectra of Figs. 5–8 appear at approximately the same energy (~13 and ~20 eV), have about the same width, their position do not depend on projectile type, energy, or orientation of the sample, suggesting strongly the same origin. In support of this assignment we note that the width of these structures, in particular that at 20 eV which is better defined, is similar to the width of the corresponding structure in the calculated loss function.[53] As mentioned above, the excitation of interband transitions contribute to the whole double peaked structure of the loss function,[53] and therefore we cannot exclude direct interband excitations (nonmediated by plasmons) in the spectrum of low energy electrons. In fact, the coexistence of these interband transitions with states at 23 eV above the Fermi energy (requiring 25 eV of excitation energy) and the collective mode at energies around 27 eV, may explain the dominance of the peak around 20 eV over the one at 13 eV.

Finally, concerning the structures seen between 30 and 55 eV we first note that they are very small, which makes their

identification difficult because they are subject to variations due to the spectrum statistics. However, the spectra taken at high energies always show structures in that energy range which do not move with projectile energy and that approximately scale with the Cu excitation at 20 eV and the Auger peak at 60 eV. Assuming that the 60 eV Auger electrons suffer the same energy losses as the ones observed in the loss spectra of Fig. 9, we should observe structures at the positions indicated in Fig. 8(b) by the dotted vertical lines. Since the source of electrons in this case (the Auger electrons) are not monoenergetic, i.e., the Auger peak is approximately 10 eV wide, some of the low energy losses will appear overlapped with the low energy part of the Auger peak and may be difficult to observe. The losses at 19.5 and 27 eV should be seen better. The fact that most of the small structures observed between 30 and 55 eV appear close to the predicted energies for losses in the Auger peaks [Fig. 8(b)] and that in general they are better seen when the Auger peak is intense supports this interpretation for their origin.

IV. SUMMARY

We presented a study of the interaction of H^+, H_2^+, He^+, Ne^+, and Ar^+ projectiles with single crystalline and polycrystalline Cu surfaces in the energy range from 5 to 100 keV. For Ne scattering we have observed small structures in the electron spectra that can be assigned to decay of Ne** autoionizing states. These structures have some similarities with those observed previously for Ne scattering on Na, Mg, Al, and Si targets, and some distinct features. As opposed to the Na, Mg, and Al cases these structures appear at higher projectile energies, above a few keV, and the structure associated to Ne**$2p^4(^3P)\,3s^2$ has a lower intensity than the $2p^4\,(^1D)\,3s^2$ structure. Above 10 keV we observed produc-

tion of other structures which we assigned to Ne** $2s2p^5nl$ and $2s2p^6nl$ states. We also observed that the line shapes of these peaks changes as a function of surface roughness—flattening of the surface by the grazing ion beam is sufficient to make them disappear.

The electron spectra induced by all the projectiles also show structures in the region 13–60 eV which remain in the same position with varying projectile energy and that change in intensity with projectile type and energy. These structures are less dependent on surface roughness. The most prominent of these structures appears at about 20 eV, another is seen at 13 eV, and both are also observed in electron induced spectra. A study of these structures as a function of energy and incident and observation angles allowed us to discard potential emission and diffraction effects as the main mechanisms responsible for their origin. A study of electron spectra induced by electrons in the range of 400 to 2500 eV allowed us to correlate these structures with the energy loss features due to single and collective excitations seen in Cu at 19.5 and 27 eV. Other smaller structures seen at energies between 30 and 55 eV are probably due to losses of the 60 eV Auger electrons of Cu.

[1] G. Zampieri, F. Meier, and R. Baragiola, Phys. Rev. A **29**, 116 (1984).

[2] S. Kasi, H. Kang, C. S. Sass, and J. W. Rabalais, Surf. Sci. Rep. **10**, 1 (1989).

[3] O. Grizzi, M. Shi, H. Bu, J. W. Rabalais, and R. A. Baragiola, Phys. Rev. B **41**, 4789 (1990).

[4] T. E. Gallon and A. P. Nixon, J. Phys. C **4**, 9761 (1992).

[5] S. Valeri, Surf. Sci. Rep. **17**, 85 (1993).

[6] S. Lacombe, V. A. Esaulov, L. Guillemot, O. Grizzi, M. Maazouz, N. Mandarino, and Vu Ngoc Tuan, J. Phys.: Condens. Matter **7**, L261 (1995).

[7] F. Xu, N. Mandarino, A. Oliva, P. Zoccali, M. Camarca, A. Bonanno, and R. A. Baragiola, Phys. Rev. A **50**, 4040 (1994).

[8] L. Guillemot, S. Lacombe, M. Maazouz, Vu Ngoc Tuan, V. A. Esaulov, E. A. Sánchez, Y. Bandurin, A. Daschenko, and V. Drobnich, Surf. Sci. **365**, 353 (1996).

[9] O. Grizzi, E. A. Sánchez, J. E. Gayone, L. Guillemot, V. A. Esaulov, and R. A. Baragiola, Surf. Sci. **469**, 71 (2000).

[10] T. M. Buck, W. E. Wallace, R. A. Baragiola, G. H. Wheatley, J. B. Rothman, R. J. Gorte, and J. G. Tittensor, Phys. Rev. B **48**, 774 (1993).

[11] Ting Li and R. J. Mac Donald, Phys. Rev. B **51**, 17 876 (1995).

[12] H. Raether, *Excitation of Plasmons and Interband Transitions by Electrons* (Springer, Berlin, 1980).

[13] D. Hasselkamp and A. Schamann, Surf. Sci. **119**, L388 (1982).

[14] M. Rösler, Nucl. Instrum. Methods Phys. Res. B **78**, 263 (1993).

[15] D. L. Mills, Surf. Sci. **294**, 161 (1993).

[16] M. Rocca, Surf. Sci. Rep. **22**, 1 (1995).

[17] R. A. Baragiola and C. A. Dukes, Phys. Rev. Lett. **76**, 2547 (1996).

[18] S. R. Barman, P. Häberle, and K. Horn, Phys. Rev. B **58**, R4285 (1998).

[19] S. M. Ritzau, R. A. Baragiola, and R. C. Monreal, Phys. Rev. B **59**, 15 506 (1999).

[20] R. A. Baragiola, S. M. Ritzau, R. C. Monreal, C. A. Dukes, and P. Riccardi, Nucl. Instrum. Methods Phys. Res. B **157**, 110 (1999).

[21] E. A. Sánchez, J. E. Gayone, M. L. Martiarena, O. Grizzi, and R. A. Baragiola, Phys. Rev. B **61**, 14209 (2000).

[22] G. Chiarello, V. Formoso, A. Santaniello, E. Colavita, and L. Papagno, Phys. Rev. B **62**, 12 676 (2000).

[23] N. Stolterfoht, D. Niemann, V. Hoffmann, M. Rösler, and R. A. Baragiola, Phys. Rev. A **61**, 052902 (2000).

[24] M. Rösler, Nucl. Instrum. Methods Phys. Res. B **164–165**, 873 (2000).

[25] B. van Someren, P. A. Zeijlmans van Emmichoven, I. F. Urazgil'din, and A. Niehaus, Phys. Rev. A **61**, 32902 (2000); H.-J. Hagemann, E. Gudat, and C. Kunz, Optical Constants from the Far Infrared to the X-ray region: Mg,Al,Cu,Ag,Au,Bi,C and Al (Deutsches Elektronen-Synchroton Report No. DESY SR-74/7, Hamburg, 1974) (unpublished); J. Opt. Soc. Am. **65**, 742 (1975).

[26] B. van Someren, P. A. Zeijlmans van Emmichoven, I. F. Urazgil'din, and A. Niehaus, Phys. Rev. A **61**, 32902 (2000).

[27] R. A. Baragiola, C. Dukes, and P. Riccardi, Nucl. Instrum. Methods Phys. Res. B **182**, 73 (2001).

[28] H. P. Winter, H. Eder, F. Aumayr, J. Lörincik, and Z. Sroubek, Nucl. Instrum. Methods Phys. Res. B **182**, 15 (2001).

[29] A. Niehaus, P. A. Zeijlmans van Emmichoven, I. F. Urazgil'din, and van Someren, Nucl. Instrum. Methods Phys. Res. B **182**, 1 (2001).

[30] N. Stolterfoht, J. H. Bremer, V. Hoffman, M. Rösler, R. Baragiola, and I. De Gortari, Nucl. Instrum. Methods Phys. Res. B **182**, 89 (2001).

[31] N. Stolterfoht, J. H. Bremer, V. Hoffmann, M. Rösler, and R. A. Baragiola, Nucl. Instrum. Methods Phys. Res. B **193**, 523 (2002).

[32] N. Pauly, A. Dubus, and M. Rösler, Nucl. Instrum. Methods Phys. Res. B **193**, 414 (2002).

[33] Y. Bandurin, S. Lacombe, L. Guillemot, and V. A. Esaulov, Surf. Sci. **513**, L413 (2002).

[34] S. Lacombe, V. A. Esaulov, E. A. Sánchez, O. Grizzi, and N. R. Arista, Phys. Rev. B **67**, 125418 (2003).

[35] J. Fayeton, N. Anderson, and M. Barat, J. Phys. B **9**, L149 (1976).

[36] M. Maazouz, A. Borisov, V. A. Esaulov, J. P. Gauyacq, L. Guillemot, S. Lacombe, and D. Teillet-Billy, Phys. Rev. B **55**, 13 698 (1996).

[37] R. M. Chaudri and M. Y. Khan, Nature (London) **192**, 646 (1961).

[38] G. Spierings, I. F. Urazgildin, P. A. Zeijlmans van Emmichoven, and A. Niehaus, Nucl. Instrum. Methods Phys. Res. B **125**, 27 (1997).

[39] G. Spierings, PhD. Thesis, Universiteit Utrecht, the Nethrlands, 1996.

[40] L. F. De Ferrariis, F. Tutzauer, E. A. Sánchez, and R. A. Baragiola, Nucl. Instrum. Methods Phys. Res. A **281**, 43 (1989).

[41] O. Grizzi, E. A. Sánchez, L. Guillemot, and V. A. Esaulov, Phys. Rev. A **65**, 052901 (2002).

[42] V. A. Esaulov, J. Phys. C **7**, 5303 (1995).

[43] F. Louchet, L. Viel, C. Benazeth, B. Fagot, and N. Colombie, Radiat. Eff. **14**, 123 (1972).

[44] A. Niehaus, P. A. Zeijlmans van Emmichoven, I. F. Urazgildin, and B. van Someren, Nucl. Instrum. Methods Phys. Res. B **182**, 1 (2001).

[45] H. Eder, F. Aumayr, P. Berlinger, H. Stori, and HP. Winter, Surf. Sci. **472**, 195 (2001).

[46] E. A. Sánchez, O. Grizzi, G. Nadal, G. R. Gómez, M. L. Martiarena, and V. H. Ponce, Nucl. Instrum. Methods Phys. Res. B **90**, 261 (1994).

[47] G. R. Gómez, E. A. Sánchez, O. Grizzi, M. L. Martiarena, and V. H. Ponce, Nucl. Instrum. Methods Phys. Res. B **122**, 171 (1997).

[48] Z. Miskovic and R. K. Janev, Surf. Sci. **221**, 317 (1989).

[49] G. Chiarello, E. Colavita, M. De Crescenzi, and S. Nannarone, Phys. Rev. B **29**, 4878 (1984).

[50] D. L. Misell and A. J. Atkins, Philos. Mag. **27**, 95 (1973).

[51] H. Papp, Surf. Sci. **63**, 182 (1977).

[52] L. A. Feldkamp, L. C. Davis, and M. B. Stearns, Phys. Rev. B **15**, 5535 (1977).

[53] I. Campillo, A. Rubio, and J. M. Pitarke, Phys. Rev. B **59**, 12 188 (1999).

[54] H. J. Hagemann, W. Gudat, and C. Kunz (unpublished).

[55] Ming Chen Wu and P. J. Moller, Phys. Rev. B **40**, 6063 (1989).